Hindawi Publishing Corporation
International Journal of Microwave Science and Technology
Volume 2014, Article ID 862649, 12 pages
http://dx.doi.org/10.1155/2014/862649

Research Article

Low Actuation Voltage RF MEMS Switch Using Varying Section Composite Fixed-Fixed Beam

M. Manivannan,[1] R. Joseph Daniel,[1] and K. Sumangala[2]

[1] *NPMaSS MEMS Design Centre, Department of Electronics and Instrumentation Engineering, Annamalai University, Annamalai Nagar, Tamilnadu 608002, India*
[2] *Department of Civil and Structural Engineering, Annamalai University, Annamalai Nagar 608002, India*

Correspondence should be addressed to R. Joseph Daniel; josuma.au@gmail.com

Received 29 May 2014; Revised 10 September 2014; Accepted 19 September 2014; Published 20 October 2014

Academic Editor: Giancarlo Bartolucci

The present authors have earlier reported the employment of varying section fixed-fixed beam for achieving lower pull-in voltage with marginal fall in restoring force. Reducing Young's modulus also reduces the pull-in voltage but with lesser degree of reduction in restoring force. Composite beams are ideal alternatives to achieve decreased Young's modulus. Hence new varying section composite fixed-fixed beam type RF MEMS switch has been proposed. The main advantage of this RF MEMS switch is that lower pull-in voltages can be achieved with marginal fall in stiction immunity. Spring constant of the proposed switch has been obtained using simulation studies and it has been shown that the spring constant and therefore the pull-in voltage (V_{pi}) can be considerably reduced with the proposed switch. Simulation studies conducted on the proposed switch clearly demonstrate that the pull-in voltage can be reduced by 31.17% when compared to the varying section monolayer polysilicon fixed-fixed beam. Further this approach enables the designer to have more freedom to design lower pull-in voltage switches with improved stiction immunity.

1. Introduction

At present RF MEMS devices are gaining popularity due to their appreciable performance at RF and microwave frequencies unlike their semiconductor counterparts and this has led to the growth of RF MEMS switching devices which are much closer to ideal switches [1–12]. However, most micromachined switches use electrostatic pull-in [13, 14] for the control of switching action and their main drawback is high pull-in voltage (V_{pi}) against the current trend of using low voltage power supplies which makes them useless in miniaturized mobile systems. In the last decade researchers worldwide have been focusing their effort to design switches with lower pull-in voltage. Three different approaches have been employed generally by researchers, namely, reducing the air gap, increasing the electrostatic actuation area, and decreasing the stiffness constant by either increasing the length or reducing the width [3, 15–19]. Among these three, the third approach is widely attempted. This approach depends on decreasing spring constant of the beams by increasing the beam length (L) and/or reducing the beam width (W) but ensuring that the beam does not show the tendency to stiction with the surface. In other words reduction in pull-in voltage must be achieved without any serious loss of restoring force (F_R). Hence it becomes necessary to find an approach where pull-in voltage is reduced but with minimum loss of F_R.

The present authors have earlier reported the employment of varying section fixed-fixed beam for achieving lower pull-in voltage [20–23] with marginal fall in restoring force. Simple calculations would show that reducing Young's modulus also reduces the pull-in voltage but with lesser degree of reduction in restoring force. Composite beams can be modelled into a single material beam of low effective Young's modulus [20, 24–26] and therefore can be substituted in situations where low Young's modulus is needed. Composite beams of polysilicon [27] and aluminium have been considered in this work to verify this proposed approach. First the authors present the simulation results on fixed-fixed beams employed RF MEMS switches and compare the

results with the one obtained with mathematical modelling. Subsequently, the varying section beams reported earlier by the present authors [20–23] and shown to have reduced pull-in voltage with marginal loss of F_R have been made composite beams to realize RF MEMS switches with still smaller pull-in voltage but with better stiction immunity. In addition to this the switching characteristics and temperature effects have also been studied to demonstrate the usefulness of the proposed switches. Further the study has been extended to evaluate the reliability of the switches considered in this study.

2. Material Selection for MEMS Switches

Since stiction has become the main concern for the RF MEMS switch reliability, considerable research effort has been directed to reduce or completely get rid of this problem. The material properties assume a very important role in the prevention of stiction. This section discusses the selection of appropriate material for the beam structure.

2.1. Selection of Contact and Bridge Material. The selection of contact metal depends on material hardness, resistivity, melting point, and process difficulty. Material properties vary significantly based on the deposition condition of material. The resistivity of a sputtered metal film is almost twice its bulk resistivity. Pure Au provides the lowest contact resistance and is most inert to oxidation but the predominant failure mechanism of pure Au contacts was found to be contact pitting and hardening damage of contact area due to repetitive contact. Hence, pure Au is not suitable for RF switch applications that require long cycling lifetime. On the other hand, hard metals like tungsten and molybdenum handle relatively large power and do not show any stiction issue but they too have their share of problems as they were found to be more sensitive to oxidation and requirement of relatively high initial contact force. Thus, tungsten and molybdenum are not suitable as contact materials. From the established results evaporated aluminium is found to be one of the suitable candidates as contact material [28].

A variety of materials are available to be used as bridge material in RF MEMS switches. Some of the most common materials used as bridge material for both cantilever and fixed-fixed beam switches are gold, aluminum, platinum, molybdenum, nickel, and copper.

To select the best possible material, three primary performance indices namely pull-in voltage, RF_{Loss} and thermal residual stress, are considered. The various material properties, such as Young's modulus (E), Poisson's ratio (ν), thermal expansion coefficient (α), thermal conductivity (K), and electrical resistivity (ρ), determine the above mentioned performance indices.

This pull-in voltage is given by [9]

$$V_{pi} = \sqrt{\frac{8kg_0^3}{27\varepsilon_0 A}}, \quad (1)$$

where k is the spring constant in N/m, g_0 is the initial gap in μm, ε the permittivity, and A is the electrostatic area in μm^2.

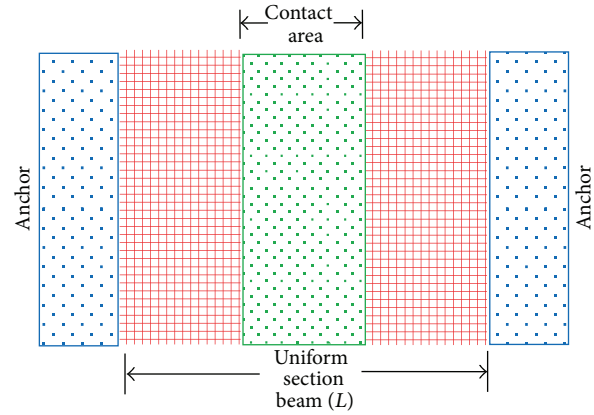

Figure 1: Top view of the RF MEMS switch employing uniform fixed-fixed beam.

The spring constant depends on Young's modulus, thermal residual stress, and Poisson's ratio of bridge material. Hence pull-in voltage of MEMS switch can be optimized by selection of a material with appropriate values of above mentioned properties.

Second performance index is related to the RF loss which can be reduced significantly by choosing suitable bridge material having good conductivity. RF power dissipated in the beam is given by [29]

$$P_{loss} = I^2 R, \quad (2)$$

where I is the current in the switch beam and R is the beam resistance.

For large RF signals, the MEMS bridge experiences the temperature change due to self-heating which further causes the change in thermal residual stress which is given by [29]

$$\Delta\sigma = E\Delta\alpha P_{loss} R_{TH}, \quad (3)$$

where P_{loss} is RF power loss and R_{TH} is thermal resistance.

The thermal resistance depends on the thermal conductivity. Hence, by selection of material with desired properties, optimum performance of MEMS switch can be obtained. Based on material selection charts [30] it is observed that aluminium is the best possible candidate as bridge structural material followed by nickel and copper. Based on these observations the authors have considered aluminium in this research work.

3. Structure of the Uniform Section Fixed-Fixed Beam Type RF MEMS Switches

Fixed-fixed beams are commonly used due to their relatively high spring constant and ease of manufacturing.

Higher value of spring constant lowers the switching time but leads to larger pull-in voltage. Due to other advantageous factors such as greater stability and lower sensitivity to stress, the fixed-fixed beam is usually the preferred choice for the membrane.

The top view of the RF MEMS switch employing uniform section fixed-fixed beam is shown in Figure 1 with beam

Table 1: Spring Constant Values.

Beam Length (μm)	Spring Constant Values		% Error
	Analytical (1)	Simulated (2)	
150	334.5	324	3.1
225	98.16	99.11	0.1
300	41.81	41.61	0.05

length $L = 150\,\mu$m, width $W = 50\,\mu$m, and air gap $2\,\mu$m. The contact area is having length equal to one third of the total beam length. Here the structural material under consideration is polysilicon. In this study electrostatic actuation is considered for the well-known advantages of this technique. The residual stress is assumed to be zero in all the simulations but in actual fabricated devices its effect cannot be neglected.

3.1. Estimation of Spring Constant. Lower pull-in voltage without impairing the restoring force too significantly is the main purpose of suspended structures that have low spring constant [20]. Deflection per unit load is termed as spring constant. For a fixed-fixed beam membrane, the spring constant can be modeled with the expression [7]

$$k = 17.64EW\left[\frac{t}{L}\right]^3, \tag{4}$$

where E is Young's modulus of the material of the beam, W is its width, t is its thickness, and L is its length.

It is important to note from this expression that the spring constant is a direct function of Young's modulus of the material of the beam. The midpoint deflection is obtained using TEM module of IntelliSuite software for a given pressure load. The effective spring constant k_{eff} is estimated using (5) obtained from simulation using IntelliSuite:

$$k_{\text{eff}} = \frac{P}{\delta_{\max}}, \tag{5}$$

where P is the force and $\delta_{\max}$ is the midpoint deflection. The spring constant values thus obtained are summarized in Table 1 for three different lengths of the beam.

The comparison of the spring constants estimated analytically using (1) and the spring constants obtained using the deflection (2) obtained in the thermoelectromechanical relaxation analysis shows that these values closely match.

3.2. Estimation of Pull-In Voltage and Restoring Force. The pull-in voltage of an electrostatically actuated fixed-fixed beam is given by (1) [9].

Restoring force (F_R) is a mechanical force component that is responsible for making the beam to assume its unbiased position upon removal of the applied bias, since it always counters electrostatic force. This is expressed by

$$F_R = kg, \tag{6}$$

where k is the spring constant in N/m and g is the central deflection in μm.

The pull-in voltages are calculated with (3) using the stiffness constants obtained analytically and by simulation in the previous section. Further the pull-in voltages are also estimated using electrostatic analysis conducted on the switches using IntelliSuite MEMS design tool. Here the actuation voltage required to cause a midpoint deflection of one third of the unbiased air gap (g_0) is considered to be the pull-in voltage as usual. The results are presented in Table 2 for immediate reference and these values are found to match closely.

Also the deflection response of the uniform section fixed-fixed polysilicon beam switch is shown in Figure 2, where the curve with solid symbol represents relationship between applied voltage and distance to travel ($g_0 - g$), while the plot with open symbol represents the relationship between applied voltage and restoring force. For the deflection equal to $(1/3)g_0$, the increase in the electrostatic force is greater than the increase in the restoring force, resulting in the beam position becoming unstable and collapse of the beam to the down-state position. These three pull-in voltages obtained for three different devices with beam lengths of 150 μm, 225 μm, and 300 μm are summarized in Table 2. The optimised grid and mesh sizes were 5 μm which ensures the least error. It can be observed from Table 2 that when the beam length increases from 150 μm to 225 μm, the spring constant gets reduced to 99.11 N/m and there is a fall in restoring force by 69%. Further increase in beam length to 300 μm makes the spring constant drop to 41.81 N/m which in turn pulls down the restoring force by 87%. It is obvious from these results that pull-in voltage falls by 4.5 times and the restoring force falls by 7.9 times when the length is doubled. Further the estimated pull-in voltages by all the three approaches closely match thus proving that the simulation results are accurate with negligible error.

Hence it is evident that manipulating the geometries of uniform section polysilicon beam is not a viable method for designing lower pull-in voltage with nominal restoring force. A possible alternative approach is reducing Young's modulus (4) and (1) instead of length. In order to further analyse the effect of fall in pull-in voltage and restoring force when Young's modulus is manipulated rather than the device geometries the authors have conducted simulation studies on single material beam for various lengths and various Young's modulus. The results are plotted as shown in Figures 3(a), 3(b), and 3(c). There are two curves and the first curve shows the spring constant estimated for the beam length in the range of 150 to 300 μm with Young's modulus equal to 160 GPa. The second curve is obtained for Young's modulus in the range 180 GPa to 10 GPa and the length is assumed to be 150 μm. It is clear from Figure 3(a) that the fall in spring constant is linear with fall in Young's modulus and the spring constant falls at smaller rate compared with the spring constant. Also it is seen from the curve 2 of Figures 3(b) and 3(c) that the pull-in voltage falls by 1.4 times when the restoring force just falls by a factor of 2, when Young's modulus is reduced by half. Therefore manipulating Young's modulus has its own advantages. All the discussions presented here assume central actuation and the pull-in voltages have been calculated for centrally actuated fixed-fixed beams. However considering

Table 2: Uniform Section Fixed-Fixed Beam Parameters.

Beam Length (μm)	Electrostatic Area (μm^2)	Restoring Force (μN)	Pull-in Voltage (Volts)			% Error
			Analytical (1)	Simulated (2)	Electrostatic Analysis	
150	2500	213.74	189.23	186.22	202.5	6.5
225	3750	65.41	84.11	83.71	87	3.3
300	5000	27.59	47.31	47.2	49.9	5.1

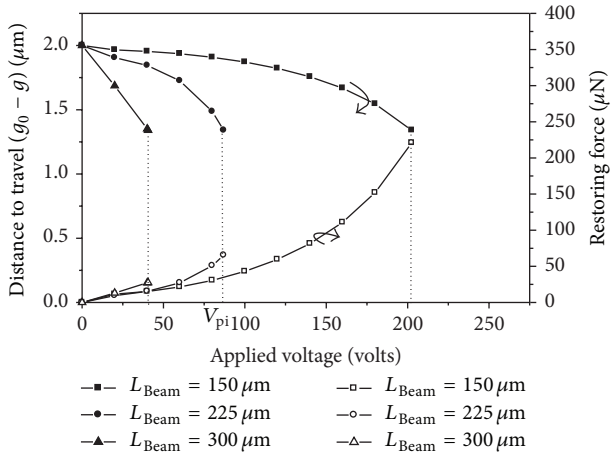

Figure 2: Actuation voltage versus displacement and restoring force of devices.

the necessity to separate the RF and DC paths, lateral actuation in the place of central actuation is chosen in actual devices. By properly choosing the shape and the dimensions of the structure, the actuation occurs without having the bridge touching the lateral actuation pads. However, the pull-in voltage would be larger and it can be even an order more as reported by Marcelli et al. [31], since the spring constant is higher for lateral actuation and this issue can be resolved by the method adopted by Marcelli et al. [32].

4. Structure of the Uniform Section Composite Fixed-Fixed Beam Type RF MEMS Switches

The studies on the uniform beams employed resistive switches in the previous sections have clearly illustrated that the IntelliSuite MEMS CAD tool can give accurate results. Further it has been demonstrated by the same analysis in the previous sections that manipulating Young's modulus can result in lower pull-in voltage without impairing the restoring force much. But Young's modulus is a material property and therefore it is constant for any given material. Either a new material or an alloy must be found out which can be a difficult task. Therefore the present authors introduce an indirect method that can be an alternative to a new material or alloy. Composite beam is the choice of the authors for the following reason. Composite beams are formed by depositing two or more layers of different materials that have different Young's modulus and thicknesses. In such a situation, composite beam can be modelled as a new single material beam with an equivalent Young's modulus, thus solving our problem.

Composite beams are expected to reduce pull-in voltage without much fall in restoring force, since Young's modulus is manipulated. The length and width of the switch are kept the same ($L_{\text{Beam}} = 150\,\mu$m, $W_{\text{Beam}} = 50\,\mu$m) as the first device described in Section 3. The thickness of the three layers of metal, polysilicon, and metal constituting the composite beam have been chosen as 0.4 μm, 1.2 μm, and 0.4 μm, respectively. It is important to note that the 2 μm thick polysilicon beam is now replaced by the composite beam as said above.

The cross-sectional view of the RF MEMS switches employing uniform section composite fixed-fixed beam is shown in Figure 4. As it is seen in the figure, the single material uniform section fixed-fixed beam is replaced by a composite fixed-fixed uniform section beam of polysilicon and aluminium with the polysilicon layer sandwiched between the top and bottom layers of aluminium. With simulation studies using thermoelectromechanical (TEM) module of IntelliSuite software the pull-in voltage for the structure shown in Figure 4 with beam length 150 μm, width 50 μm, and air gap 2 μm was found to be 158.25 volts. The next section presents the theoretical analysis and attempts to validate the proposed approach.

4.1. Theoretical and Thermoelectromechanical Relaxation Analysis of Uniform Section Composite Beam Switches. The composite beams analysis has been carried out by transforming this beam into a single material beam with an effective Young's modulus and effective Poisson's ratio. The effective Young's modulus is estimated using the expression [24]

$$E_{\text{eff}} = \frac{E_{\text{Al}}A_{\text{Al}} + E_{\text{Poly}}A_{\text{Poly}}}{A_{\text{Al}} + A_{\text{Poly}}}. \tag{7}$$

The equivalent density is given by expression [24]

$$\rho_{\text{eff}} = \frac{\rho_{\text{Al}}A_{\text{Al}} + \rho_{\text{poly-Si}}A_{\text{poly-Si}}}{A_{\text{Al}} + A_{\text{poly}}}. \tag{8}$$

The equivalent thickness is also obtained from the equivalent density equation

$$T_{\text{eff}} = \frac{m_{\text{eff}}}{\rho_{\text{eff}} * L_{\text{eff}} * W_{\text{eff}}}, \tag{9}$$

where E_{Al} is Young's modulus of aluminium, E_{Poly} is Young's modulus of polysilicon, "A" is cross-sectional area, m_{eff} is

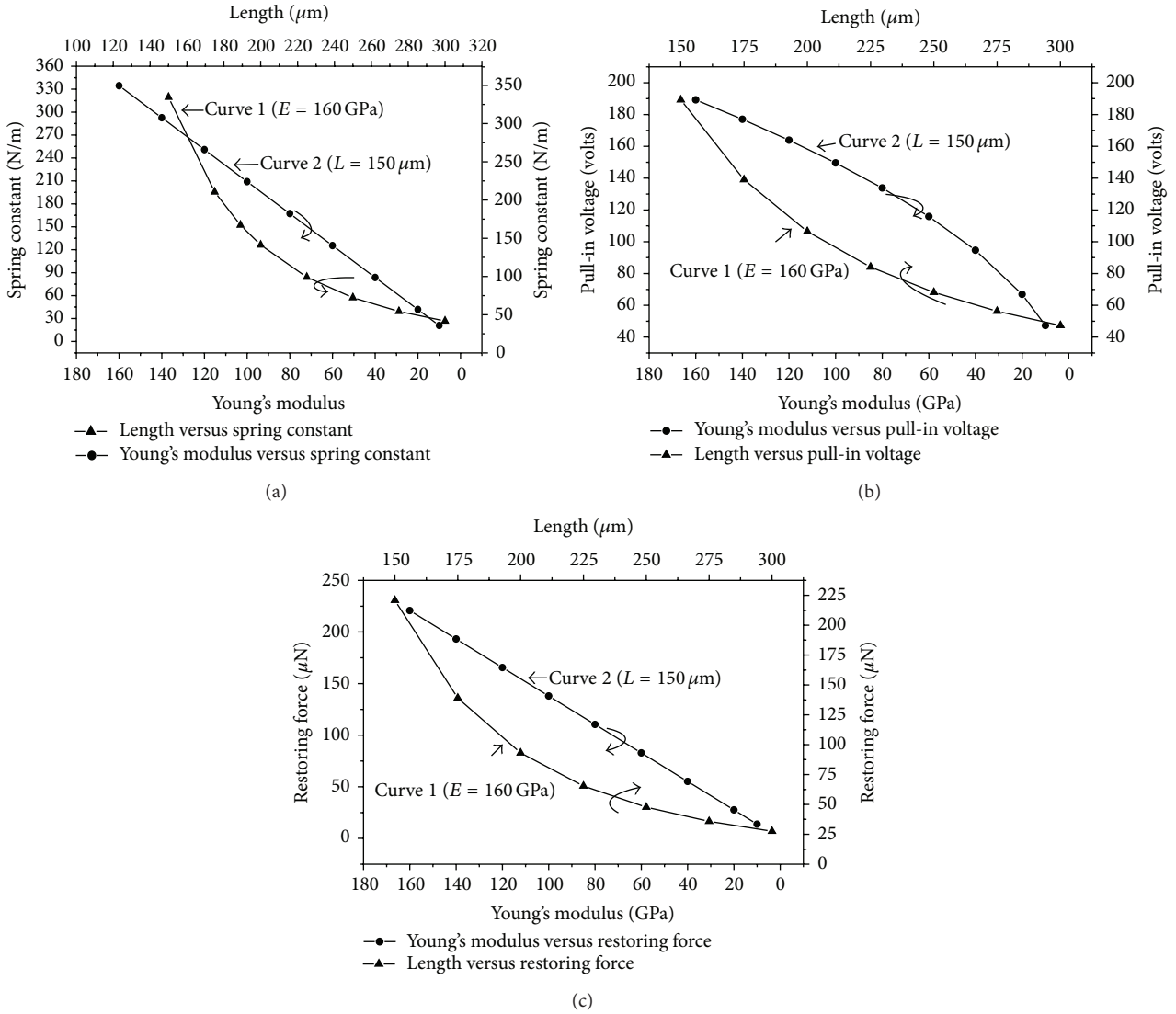

Figure 3: (a) Young's modulus, length versus spring constant. (b) Young's modulus, length versus pull-in voltage. (c) Young's modulus, length versus restoring force.

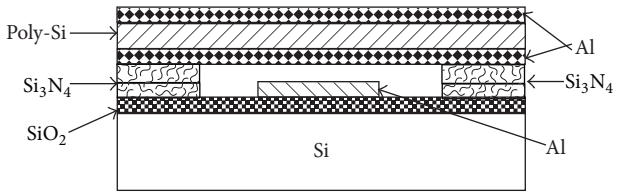

Figure 4: Cross-sectional view of the uniform section composite fixed-fixed beam type RF MEMS switch.

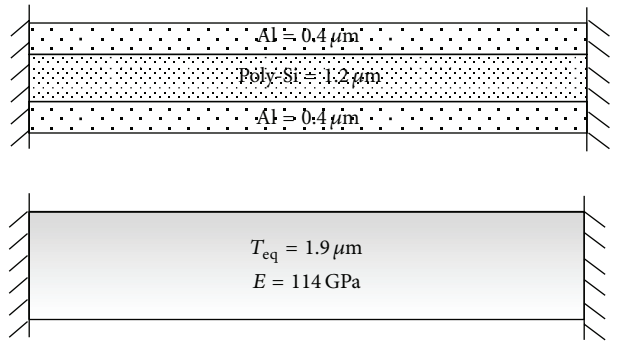

Figure 5: Composite beam and its equivalent single material beam.

effective mass, and ρ_{eff} is effective density. The single material beam equivalent to the composite (Al-Poly Si-Al) beam is shown in Figure 5. Both of the beams are of same length and width. The deflection responses of the devices are shown in Figure 6. The results clearly show that the pull-in voltage of the composite beam and its equivalent single material beam are falling in line with less than 5% error. The simulated values of pull-in voltages of the composite beam switches and the switches with their equivalent single material beam with lengths 150 μm and 300 μm are presented in Table 3.

Therefore the composite beam can be used in situations where the manipulation of Young's modulus is required.

Table 3: Estimated Device parameters.

Uniform Beam Type	Beam Length (μm)	Young's Modulus (GPa)	V_{pi} (V)	% Error
Composite	150	Al = 68.85 Poly-Si = 160	158.25	5%
Equivalent Single Material	150	114	166.3	
Composite	300	Al = 68.85 Poly-Si = 160	39.85	3.8%
Equivalent Single Material	300	114	41.37	

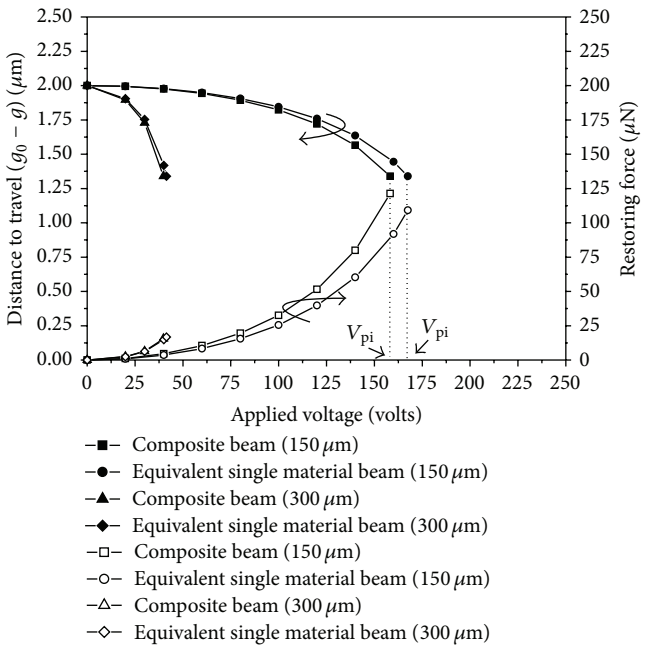

Figure 6: Actuation voltage versus displacement, restoring force of devices.

Polysilicon and aluminium are ideal candidates to form composite beams that can offer low Young's modulus and it is easier to get these films deposited by standard semiconductor fabrication process. The composite beam of length 150 μm results in a pull-in voltage of 158.25 volts (Table 3) when the single material polysilicon beam of same length gave a pull-in voltage of 202.5 volts (Table 2) in thermoelectromechanical relaxation analysis. The restoring force for the composite beam was 110 μN whereas it is 213.7 μN for polysilicon beam. The restoring force of the composite beam is larger than the restoring force that was achieved by manipulating the length/width (Table 2) of the single material beam. Hence it is again proved that the manipulation of Young's modulus is an effective method to reduce pull-in voltage with lesser extent of fall in restoring force.

At this point it is important to study the thermal behavior of composite beam MEMS switches, because polysilicon beam is now replaced by composite beam of metal-polysilicon-metal films. Polysilicon has excellent resistance to temperature effects and the replacement of composite beam should not deteriorate the thermal stability. The following section discusses the effect of temperature on the stress component of the beam.

4.2. Effect of Residual Stress and Temperature on Pull-In Voltage in Composite Beams. The other most important parameters that influence the pull-in voltage are the residual stress and the thermal expansion coefficient of the beam material. In the case of composite beams the thermal expansion coefficients of the various layers have to be taken into account. The residual stress and the stress due to thermal factors also control the spring constant and therefore the pull-in voltage. The effective spring constant of fixed-fixed beams is given by $k_{\text{total}} = k_1 + k_2$, where the k_1 component is due to the stiffness of the bridge which is determined by material characteristics such as Young's modulus and the moment of inertia. The k_2 component is due to residual stress in the beam and is controlled by the fabrication process and stress due to temperature. For a fixed-fixed beam membrane, the spring constant can be written as [7]

$$k = 17.64EW\left[\frac{t}{L}\right]^3 + 8\sigma(1-\nu)W\left[\frac{t}{L}\right]\left[\frac{3}{5}\right], \quad (10)$$

where E is Young's modulus, W is the beam width, t is the beam thickness, L is the beam length, ν is the Poisson ratio, and σ is the residual stress. The stress σ is the sum of the room-temperature built-in stress σ_i resulting from the film deposition process and a thermal stress σ_t from heating of the beam; that is,

$$\sigma = \sigma_i + \sigma_t = \sigma_i - \alpha E \Delta T, \quad (11)$$

where α is the thermal expansion coefficient and ΔT is the increase in temperature of the beam.

For a composite beam, the stress must be replaced by effective value that represents weighted averages of the different materials used, each of which has a cross-sectional area A_j. The effective stress [32, 33] is represented by (12). For a generic multilayer with N materials, one should have

$$\sigma = \sigma_{ij} - \alpha_j E_j \Delta T, \quad (12)$$

where $j = 1, 2, \ldots, N$, and

$$\langle\sigma\rangle = \frac{\sum_j A_j \sigma_j}{A} = \frac{\sum_j A_j \sigma_{ij}}{A} - \Delta T \frac{\sum_j A_j \sigma_j E_j}{A}. \quad (13)$$

In this work the effect of temperature on stress, spring constant, and pull-in voltage has been estimated using (12)

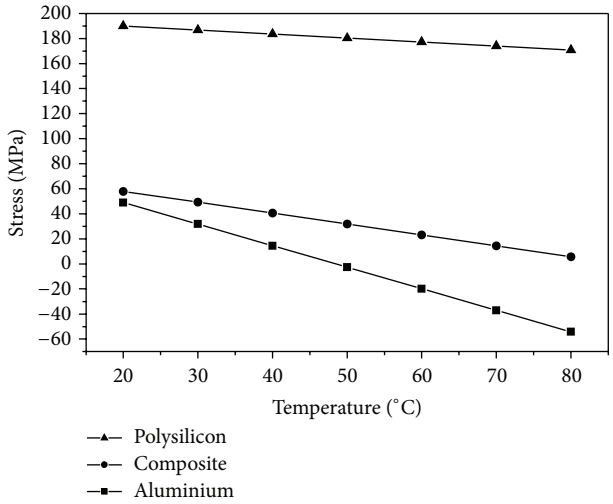

Figure 7: Temperature versus stress.

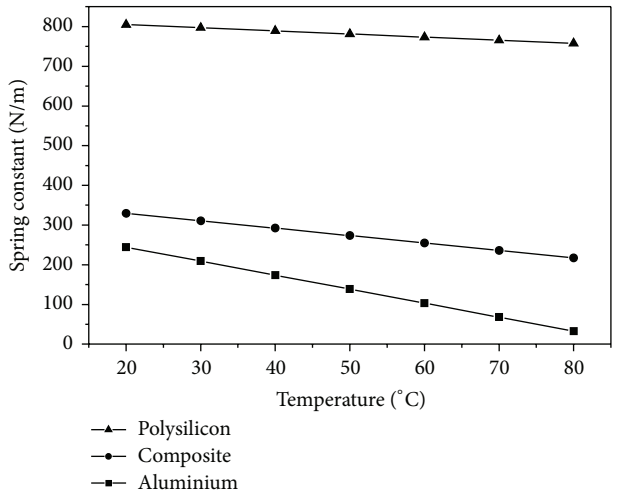

Figure 8: Temperature versus spring constant.

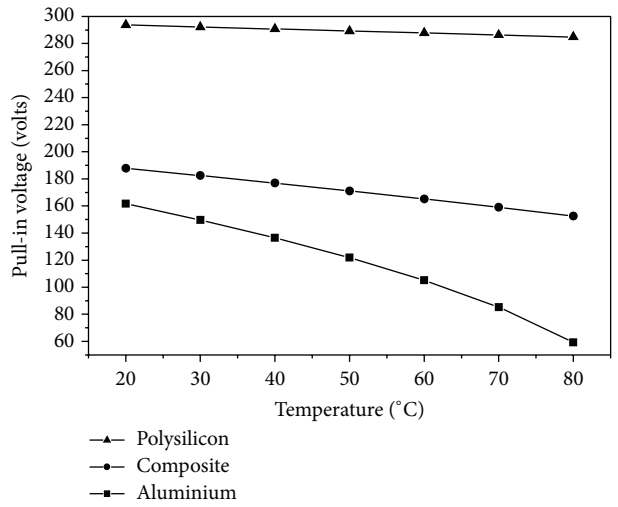

Figure 9: Temperature versus pull-in voltage.

as suggested by Marcelli et al. [31] and the results are plotted in Figures 7, 8, and 9. Initial stresses are assumed to be 49 MPa [34] and 190 MPa [35], respectively, for aluminium and polysilicon.

It may be observed from the above plots (Figures 7–9) that there is a fall in σ by 0.32, 0.87, and 1.72 MPa/°C as temperature increases from 20°C to 80°C while for the same temperature range there is a fall in k by 0.792, 1.87, and 3.52 N/m/°C, respectively, for polysilicon, composite, and aluminium beam and the pull-in voltage is found to get reduced by 0.145, 0.54, and 1.2 V/°C for polysilicon, composite, and aluminium beams, respectively. The results show that the polysilicon beams have the best thermal characteristics with least dependency of pull-in voltage on temperature. The beam made of aluminium metal alone has smaller pull-in voltage but has strong dependency on temperature. But the composite beams give moderate performance under various temperatures and with different choices of materials it is possible to further improve the temperature behaviour and trade-off performance can be achieved.

4.3. Switching Speed and Reliability of Composite Beam Switches. The other important performance factors of RF MEMS switches are the switching time and reliability. In the previous section the temperature effects on the performance of composite beams were studied and this section analyses the switching performance and reliability of composite beam switches. The electrostatic actuation is the preferred actuation mechanism in RF MEMS switches for the reasons stated in Section 2. Hence electrostatic actuation is considered here too.

4.3.1. Estimation of Switching Speed. The switching time of an electrostatically actuated RF MEMS switch strongly depends on the applied voltage. In most cases the applied voltage is 1.3-1.4 times of the pull-in voltage to obtain smaller switching time. A very large switching voltage will result in stronger electrostatic force thus leading to poor reliability. The angular frequency of any system modelled as spring is given by

$$\omega = \sqrt{\frac{k}{m}}, \tag{14}$$

where k is the spring constant and m is the mass, leading to the frequency of operation of the RF MEMS switch to be

$$f = \frac{1}{2\pi}\sqrt{\frac{k}{m}}. \tag{15}$$

Further the expression for the switching time of the RF MEMS switches with $Q \geq 2$ is given by [7, 36, 37]

$$t_s = 3.67\frac{V_{\text{pi}}}{V_s}\sqrt{\frac{m}{k}}. \tag{16}$$

The switching times of the RF MEMS switches considered in this study were evaluated using the above expressions and are

Table 4: Switching Time of the devices.

Fixed-Fixed Beam Material	Q	Switching Time (μsec)	Mass ($\times 10^{-11}$ Kg)
Aluminium	3.12	0.77	1.4175
Composite	2.80	0.70	1.3126
Polysilicon	2.22	0.59	1.2075

presented in Table 4 for immediate reference. Of the three switches studied polysilicon possesses the least switching time because of lesser mass for the given dimensions. The switching time of composite beam is neither high nor low and the aluminium beam possesses the highest switching time among three. Hence composite beams give a trade-off performance.

4.3.2. Reliability of Composite Beam Switches. The presence of mechanical contact in RF MEMS switches introduces reliability issues, related to both mechanical and electrical phenomena. Probably the most important effect impairing device functionality is the "stiction" of the mechanical parts that reached contact, which is the inability to restore a resting position after the actuation stimulus has been removed. Since pull-in voltage is reduced without impairing the restoring force in composite beams these switches are more reliable.

5. Structure of the Varying Section Fixed-Fixed Beam MEMS Switches

In the previous section it has been shown that composite beams can be used to reduce pull-in voltage without affecting F_R seriously. The authors in their earlier reports have already shown that varying section single material fixed-fixed beams can be used to achieve lower pull-in voltage still not compromising the stiction immunity much [20–23]. In the simulation studies reported by the authors earlier it has been demonstrated that the pull-in voltage can be reduced by 22.74% from that of a uniform section beam with employment of varying section beams. Therefore it is a definite possibility to achieve still better performance if these two effects are combined. The top view of the proposed RF MEMS switch employing varying section composite fixed-fixed beam is shown in Figure 10.

As it is seen in the figure, the constant width fixed-fixed beam is replaced by a varying section composite fixed-fixed beam with its wider section at the anchored ends and its narrowest section at point of contact with the contact electrode. The section closer to the anchor is of width W_1 and width of the subsequent section towards the pull-in pad assumes varying widths W_2, W_3, and so on depending on the number of sections. The length of each section is kept the same. Here "L" is the length of the beam and "n" is the number of sections on either sides of the contact area.

5.1. Pull-In Voltage and Restoring Force of Varying Section and Uniform Beam RF MEMS Switches. The authors have already reported that varying section beam employed RF

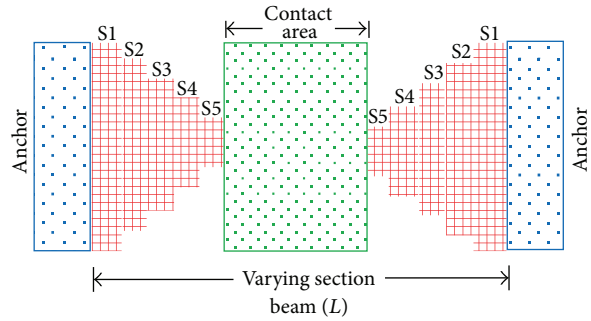

Figure 10: Top view of the proposed varying section composite fixed-fixed beam ($n = 5$).

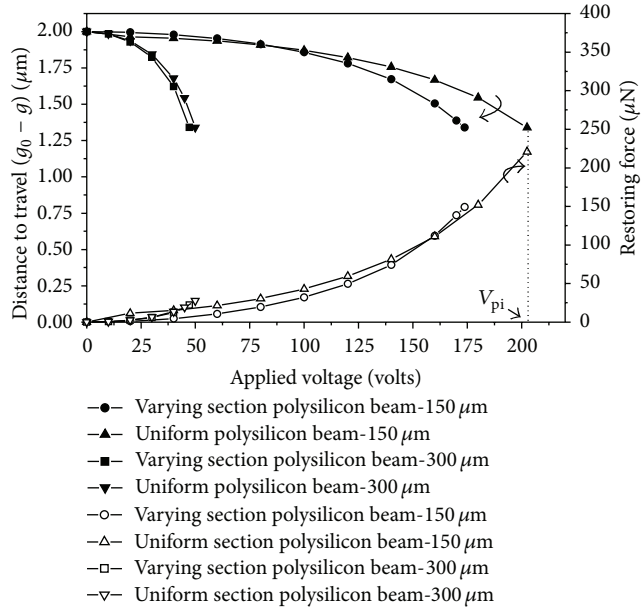

Figure 11: Actuation voltage versus displacement, restoring force.

switches can give lower pull-in voltages. The electrostatic analysis on the uniform section beams of length 150 μm and 300 μm and varying section beams of same length have been plotted here in Figure 11. These curves illustrate that the varying section beams can effectively reduce pull-in voltage without impairing the restoring forces significantly which do not happen when the beam lengths are manipulated to reduce pull-in voltages. The authors have demonstrated in the previous sections that composite beam can be used to achieve reduced pull-in voltages with minimum loss in the restoring force. Further it has been established that the composite beams can give optimum performance in terms of speed, thermal stability, and reliability. Hence it is obvious that the varying section composite beams would show better results.

5.2. Simulation Studies on Varying Section Composite Fixed-Fixed Beam

5.2.1. Device Geometries. IntelliSuite MEMS design software has been used for all the simulation studies of this work. The

Table 5: Device Geometry.

Beam Length (μm)	Device ID	Layer Thickness (μm)			Total Beam Thickness (μm)
		Al	Poly-Si	Al	
150	VSC1		Poly-Si		2
	VSC2	0.2	1.6	0.2	2
	VSC3	0.4	1.2	0.4	2
	VSC4	0.6	0.8	0.6	2
300	VSC5		Poly-Si		2
	VSC6	0.2	1.6	0.2	2
	VSC7	0.4	1.2	0.4	2
	VSC8	0.6	0.8	0.6	2

Table 6: Pull-in Voltages Extracted from electrostatic deflection analysis.

Device ID	Pull-in Voltage (Volts)	% reduction in V_{pi}
VSC1	173.75	—
VSC2	148.17	14.55
VSC3	129.98	25.18
VSC4	119.57	31.17
VSC5	47.21	—
VSC6	40.38	14.44
VSC7	35.48	24.71
VSC8	32.62	30.87

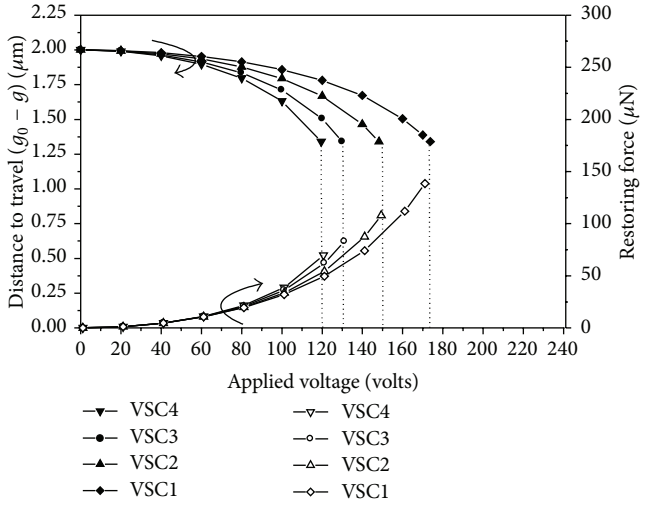

Figure 12: Actuation voltage versus displacement, restoring force of devices VSC1 to VSC4.

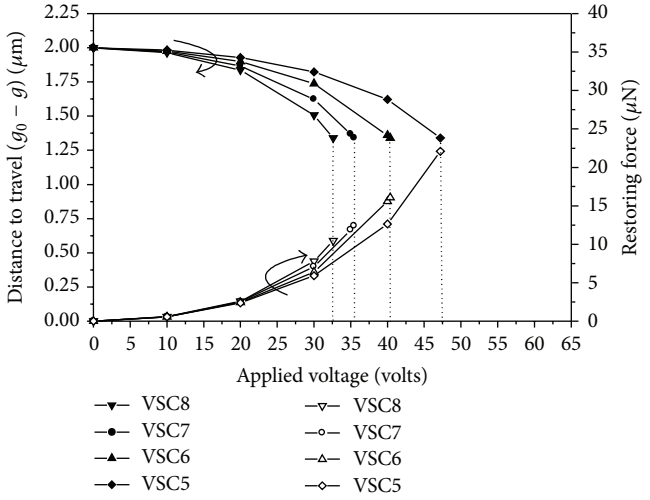

Figure 13: Actuation voltage versus displacement, restoring force of devices VSC5 to VSC8.

structure of the proposed varying section composite fixed-fixed beam type RF MEMS switch has been created using 3D builder module and thermoelectromechanical relaxation analysis has been carried out to extract the pull-in voltage. Eight different devices have been considered for simulation studies based on the beam length and thickness composition of polysilicon and aluminium. The unbiased air gap is maintained as 2 μm throughout. The beam lengths under consideration here are 150 μm and 300 μm. For all the devices, the number of sections "n" is kept at 5. The contact pad has a length of 50 μm. These dimension details along with the nomenclature followed for identifying different devices are summarized in Table 5.

5.2.2. Deflection Analysis and Extraction of Pull-In Voltage. The deflection response at various actuation voltages is obtained by observing the midpoint movement (g) towards the contact pad on application of the voltage. Thermoelectromechanical relaxation type analysis was used to achieve the goal. The deflection responses of devices under consideration are shown in Figures 12 and 13. In this graph the y-axis represents the remaining distance to be travelled ($g_0 - g$), where "g" is the deflection measured at the centre of the beam. The V_{pi} is extracted by finding the voltage at which the distance to travel ($g_0 - g$) is two thirds of the initial gap g_0 [7]. The pull-in voltage thus obtained for various devices is summarized in Table 6. It is obvious from Table 4 that there is a possibility of getting V_{pi} reduced by a maximum of around 31% with the devices VSC4 and VSC8.

In order to further validate this approach of employing varying section composite fixed-fixed beams for reducing

Table 7: Estimated Spring constant and Pull in Voltage.

Device—ID	Spring Constant (k) In N/m	Pull-in Voltage (Volts)	% Reduction		
			k	V_{pi}	F_R
VSC1	226	155.57	—	—	—
VSC2	163.4	132.29	27.69	14.55	27
VSC3	125.3	115.88	44.55	25.18	44
VSC4	105.44	106.26	53	31.17	53
VSC5	33.46	42.32	—	—	—
VSC6	24.34	36.10	27.25	14.69	27.25
VSC7	18.76	31.69	43.93	25.11	43.94
VSC8	15.83	29.10	52.73	31.23	52.7

Table 8: Comparison of Pull in Voltages.

Device	Pull in Voltage (Volts) (By Simulation)	Pull in Voltage (Volts) (Analytical)	% Error
VSC1	173.75	155.57	10.46
VSC2	148.175	132.29	10.72
VSC3	129.985	115.88	10.85
VSC4	119.575	106.26	11.13
VSC5	47.2	42.32	10.33
VSC6	40.38	36.1	11.85
VSC7	35.48	31.69	10.68
VSC8	32.65	29.1	10.87

pull-in voltage, the spring constant for all the devices was evaluated by simulation and using (2). Subsequently the pull-in voltages are assessed using (3) and are summarized in Table 7. These results demonstrate that the proposed approach reduces pull-in voltages with moderate loss of stiction immunity. From Table 7 it can be observed that a minimum of around 27% reduction in spring constant is obtainable with sacrifice of 27.25% of restoring force. Hence it is obvious that the proposed design methodology paves way for design of lower pull-in voltage RF MEMS switches with nominal restoring force. Further it can be seen from Table 8 that the error between the values of pull-in voltages of all the devices obtained by electrostatic analysis and analytical calculations is always around 10%.

6. Comparative Analysis and Discussions

The values of spring constant, pull-in voltage, and restoring force of various beams considered in this study for the given length, thickness, and electrostatic area are summarized in Table 9 for easy comparison and analysis.

The results clearly show that the composite switches are ideal for achieving trade-off between the pull-in voltage, switching time, thermal stability, and reliability. Further it shows that varying section composite beams have the advantages of reducing pull-in voltage without impairing the restoring force significantly. Finally the comparison between the devices with $L = 300\,\mu$m and $L = 150\,\mu$m clearly demonstrates that manipulating the dimensions of the device to reduce the pull-in voltage causes great loss of restoring force and the varying section composite beams proposed in this study help one to bring down the pull-in voltage with lesser extent of fall in restoring force and therefore better reliability.

7. Conclusion

The disadvantages with manipulating the dimensions of the beam to achieve lower pull-in voltage but without significantly changing the restoring force were first presented.

In this paper, the authors first propose uniform section composite beams to reduce Young's modulus and thus to realize lower pull-in voltage without compromising much on stiction immunity. A uniform section composite beam of polysilicon (160 GPa) and aluminium (68.85 GPa) and its equivalent single material (114 GPa) beam RF switches were simulated and their stiffness constant (k) and pull-in voltages are found to be closely matching, thus showing that composite beams are ideal alternative to realize lower Young's modulus. Further, this approach is also seen to reduce pull-in voltage with lesser penalty on restoring force. The present authors in their earlier reports have established that low voltage RF MEMS switches can be realized with the employment of varying section fixed-fixed beam, without impairing restoring force much. Therefore it is beneficial if the uniform composite beam is replaced by a varying section composite beam since further reduction in pull-in voltage is possible.

Hence new varying section composite fixed-fixed beam type RF MEMS switch has been proposed. The spring constant of the varying section beam considerably reduces with various thickness combinations of polysilicon and aluminium layers, thus indicating possibility of design of lower pull-in voltage RF MEMS switches using varying section composite beams. It is also seen that the appreciable reduction in k occurs for the devices VSC4 and VSC8. The comparison between theoretically estimated V_{pi} and V_{pi} extracted from simulation shows that the error is always around 10%. Presently the authors are engaged in devising a full-fledged model to bring down these deviations. However,

Table 9: Comparison of Device Parameters.

Beam Type	k (N/m)	V_{pi} (Volts)	F_R (μN)	% Reduction		
				k	V_{pi}	F_R
L_{Beam} = 150 μm, T_{Beam} = 2 μm Beam, Electrostatic area = 2500 μm^2						
Uniform Polysilicon	334.5	189.26	220.77	—	—	—
Uniform Composite	183.85	149.96	121.34	45	20.7	45
Polysilicon Varying Section	226	155.57	149.16	32.4	17.8	32.4
Composite Varying Section	125.39	115.88	82.75	62.5	38.7	62.5
L_{Beam} = 300 μm, T_{Beam} = 2 μm Beam, Electrostatic area = 5000 μm^2						
Uniform Polysilicon	41.81	47.31	27.59	—	—	—
Uniform Composite	23.5	35.5	15.51	43.7	24.9	43.7
Polysilicon Varying Section	33.46	42.32	22.08	20.2	10.5	20
Composite Varying Section	18.76	31.69	12.38	55.1	33	55.1

the analytical results fall closely and illustrate that the pull-in voltage can be reduced with the proposed structure with the varying section composite beam RF MEMS switches with marginal loss in stiction immunity. In addition to these findings the composite beams show optimum thermal characteristics and reliability.

Conflict of Interests

The authors declare that there is no conflict of interests regarding the publication of this paper.

Acknowledgment

The authors express their sincere gratitude to the NPMaSS authorities for the MEMS Simulation and Design tools provided to NPMaSS MEMS Design Centre, Annamalai University.

References

[1] G. M. Rebeiz and J. B. Muldavin, "RF MEMS switches and switch circuits," *IEEE Microwave Magazine*, vol. 2, no. 4, pp. 59–71, 2001.

[2] S. Afrang and G. Rezazadeh, "Design and simulation of simple and varying section cantilever and fixed-fixed end types MEMS switches," in *Proceedings of the IEEE International Conference on Semiconductor Electronics (ICSE '04)*, pp. 593–596, Kuala Lumpur, Malaysia, December 2004.

[3] D. Peroulis, S. P. Pacheco, K. Sarabandi, and L. P. B. Katehi, "Electromechanical considerations in developing low-voltage RF MEMS switches," *IEEE Transactions on Microwave Theory and Techniques*, vol. 51, no. 1, pp. 259–270, 2003.

[4] S. P. Pacheco, L. P. B. Katehi, and C. T.-C. Nguyen, "Design of low actuation voltage RF MEMS switch," in *Proceedings of the IEEE MTT-S International Microwave Symposium*, vol. 1, pp. 165–168, June 2000.

[5] P. Verma and S. Singh, "Design and simulation of RF MEMS capacitive type shunt switch & its major applications," *IOSR Journal of Electronics and Communication Engineering*, vol. 4, no. 5, pp. 60–66, 2013.

[6] D. Peroulis, *RF MEMS devices for multifunctional integrated circuits and antennas [Ph.D. Dissertation Electrical Engineering]*, The University of Michigan, 2003.

[7] G. M. Rebeiz, *RF MEMS Theory Design and Technology*, John Wiley & Sons, Hoboken, NJ, USA, 2003.

[8] S. Raghavan, T. Shanmuganantham, and G. Jansi Rani, "Electromechanical modelling of high power RF MEMS switches," *Journal-ET*, vol. 89, pp. 24–27, 2008.

[9] S. P. Pacheco, L. P. B. Katehi, and C. T.-C. Nguyen, "Design of low actuation voltage RF MEMS switch," in *Proceedings of the IEEE MTT-S International Microwave Symposium Digest*, 2000.

[10] J. E. Massad, H. Sumali, D. S. Epp, and C. W. Dyck, "Modeling, simulation, and testing of the mechanical dynamics of an RF MEMS switch," in *Proceedings of the International Conference on MEMS, NANO and Smart Systems (ICMENS '05)*, pp. 237–240, July 2006.

[11] J. Oberhammer, B. Lindmark, and G. Stemme, "RF characterization of low-voltage high-isolation MEMS series switch based on a S-shaped film actuator," in *Proceedings of the SMBO/IEEE MTT-S International Microwave and Optoelectronics Conference (IMOC '03)*, pp. 537–540, September 2003.

[12] R. Sha, R. Ghatak, and R. Mahapatra, "Impact of beam thickness and air gap on the performance of cantilever MEMS switch," *International Journal of Electronics & Communication Technology*, vol. 4, no. 1, 2013.

[13] E. K. I. Hamad, *Modeling, design, and optimization of radio frequency microelectromechanical structures [Ph.D. thesis]*, Institute for Electronics, Signal Processing, and Comm., University of Magdeburg, Magdeburg, Germany, 2006.

[14] J.-M. Huang, A. Q. Liu, C. Lu, and J. Ahn, "Mechanical characterization of micromachined capacitive switches: design consideration and experimental verification," *Sensors and Actuators A: Physical*, vol. 108, no. 1-3, pp. 36–48, 2003.

[15] J.-M. Huang, K. M. Liew, C. H. Wong, S. Rajendran, M. J. Tan, and A. Q. Liu, "Mechanical design and optimization of capacitive micromachined switch," *Sensors and Actuators A: Physical*, vol. 93, no. 3, pp. 273–285, 2001.

[16] Y. Mafinejad, A. Kouzani, and K. Mafinezhad, "Review of low actuation voltage RF MEMS electrostatic switches based

on metallic and carbon alloys," *Journal of Microelectronics, Electronic Components and Materials*, vol. 43, no. 2, pp. 85–96, 2013.

[17] H. Sadeghian, G. Rezazadeh, E. Malekpour, and A. Shafipour, "Pull-in voltage of fixed-fixed end type MEMS switches with variative electrostatic area," *Sensors & Transducers Magazine (S&T e-Digest)*, vol. 66, no. 4, pp. 526–533, 2006.

[18] D. Verma and A. Kaushik, "Analysis of RF MEMS capacitive switch based on a fixed-fixed beam structure," *International Journal of Engineering Research and Applications*, vol. 2, no. 5, pp. 391–394, 2012.

[19] J. Sharma and A. Dasgupta, "Effect of stress on the pull-in voltage of membranes for MEMS application," *Journal of Micromechanics and Microengineering*, vol. 19, no. 11, Article ID 115021, 2009.

[20] M. Manivannan, R. J. Daniel, and K. Sumangala, "Design optimization for low actuation voltage varying section fixed-fixed beam Type RF MEMS switch with improved stiction immunity," in *Proceedings of the 5th ISSS National Conference on MEMS, Smart Materials Structures and System*, Coimbatore, India, 2012.

[21] M. Manivannan, R. J. Daniel, C. A. Jeyasekar, and K. Sumangala, "Design of lower pull-in voltage RF MEMS switch using varying section cantilever beam," in *Proceedings of the National Workshop on Recent Advances in Micro Electro Mechanical Systems*, 2011, Varanasi, India.

[22] M. Manivannan, R. J. Daniel, and K. Sumangala, "Design of stictionfree—lower pull in voltage RF MEMS switch using varying section cantilever beam," *Advanced Materials Research*, vol. 403–408, pp. 4141–4147, 2012.

[23] M. Manivannan, R. Joseph Daniel, and K. Sumangala, "Low actuation voltage RF MEMS switch using varying section composite cantilever beam," in *Proceedings of the 6th ISSS National Conference on MEMS, Smart Materials Structures and System*, Pune, India, 2013.

[24] S. C. Jun, X. M. H. Huang, M. Manolidis, C. A. Zorman, M. Mehregany, and J. Hone, "Electrothermal tuning of Al-SiC nanomechanical resonators," *Nanotechnology*, vol. 17, no. 5, pp. 1506–1511, 2006.

[25] S. K. Waghmare, "Analysis and simulation of composite bridge for electrostatic MEMS switch," *International Journal of Emerging Technology and Advanced Engineering*, vol. 3, no. 5, pp. 387–390, 2013.

[26] Y. Liu, G. Wang, and H. Yang, "Analysis for pull-in voltage of a multilayered micro-bridge driven by electrostatic force," *Scientific Research, Engineering*, vol. 2, pp. 55–59, 2010.

[27] J. L. Botrel, O. Savry, O. Rozeau, F. Templier, and J. Jomaah, "Polysilicon high frequency devices for large area electronics: characterization, simulation and modeling," *Thin Solid Films*, vol. 515, no. 19, pp. 7422–7427, 2007.

[28] M. Tang, A. Agarwa, J. Li et al., "An approach of lateral RF MEMS switch for high performance," in *Proceedings of the Symposium on Design, Test, Integration and Packaging of MEMS/MOEMS*, Cannes-Mandelieu, France, May 2003.

[29] A. K. Sharma and N. Gupta, "Material selection of RF-MEMS switch used for reconfigurable antenna using Ashby's methodology," *Progress in Electromagnetics Research Letters*, vol. 31, pp. 147–157, 2012.

[30] O. Parate and N. Gupta, "Material selection for electrostatic microactuators using Ashby approach," *Materials and Design*, vol. 32, no. 3, pp. 1577–1581, 2011.

[31] R. Marcelli, A. Lucibello, G. De Angelis, E. Proietti, and D. Comastri, "Mechanical modelling of capacitive RF MEMS shunt switches," in *Proceedings of the Symposium on Design, Test, Integration & Packaging of MEMS/MOEMS (MEMS/MOEMS '09)*, pp. 19–22, Rome, Italy, April 2009.

[32] R. Marcelli, D. Comastri, A. Lucibello, G. de Angelis, E. Proietti, and G. Bartolucci, "Dynamics of RF micro-mechanical capacitive shunt switches in Coplanar waveguide configuration," in *Microelectromechanical Systems and Devices*, N. Islam, Ed., InTech, 2012, 10.5772/28251.

[33] G. de Pasquale, A. Somà, and T. Veijola, "Gas damping effect on thin vibrating gold plates: experiments and modeling," in *Proceedings of the Symposium on Design, Test, Integration & Packaging of MEMS/MOEMS (MEMS/MOEMS '09)*, pp. 23–28, Rome, Italy, April 2009.

[34] V. Mulloni, F. Solazzi, F. Ficorella, A. Collini, and B. Margesin, "Influence of temperature on the actuation voltage of RF-MEMS switches," *Microelectronics Reliability*, vol. 53, no. 5, pp. 706–711, 2013.

[35] http://www.memsnet.org/.

[36] S. Shekhar, K. J. Vinoy, and G. K. Ananthasuresh, "Switching and release dynamics of an electrostatically actuated MEMS switch under the influence of squeeze-film damping," in *Proceedings of the Nanotech Conference & Expo (MSM '12)*, June 2012.

[37] S. Shekhar, K. J. Vinoy, and G. K. Ananthasuresh, "Switching and release time analysis of electrostatically actuated capacitive RF MEMS switches," *Sensors and Transducers*, vol. 130, no. 7, pp. 77–90, 2011.